




Article

Potential Flood Risk in the City of Guasave, Sinaloa, the Effects of Population Growth, and Modifications to the Topographic Relief

Héctor José Peinado Guevara ¹, Mauro Espinoza Ortiz ^{2,*} , Víctor Manuel Peinado Guevara ^{1,*}, Jaime Herrera Barrientos ^{3,*} , Jesús Alberto Peinado Guevara ^{4,*}, Omar Delgado Rodríguez ⁵ , Manuel de Jesús Pellegrini Cervantes ⁶ and Moisés Sánchez Morales ⁷

- ¹ Escuela de Ciencias Económicas y Administrativas, Universidad Autónoma de Sinaloa, Guasave 81100, Mexico; hpeinado75@hotmail.com
- ² Instituto Politécnico Nacional, CIIDIR Unidad Sinaloa, Programa de Doctorado en Red en Ciencias en Conservación del Patrimonio Paisajístico, Guasave 81100, Mexico
- ³ Centro de Investigación Científica y de Educación Superior de Ensenada, Baja California (CICESE), Ensenada 22860, Mexico
- ⁴ Preparatoria Guasave Nocturna, Universidad Autónoma de Sinaloa, Guasave 81100, Mexico
- ⁵ División de Geociencias Aplicadas, Instituto Potosino de Investigación Científica y Tecnológica (IPICYT), San Luis Potosí 78216, Mexico; omar.delgado@ipicyt.edu.mx
- ⁶ Facultad de Ingeniería Mochis, Universidad Autónoma de Sinaloa, Los Mochis, Ahome 81256, Mexico; manuel.pellegrini@uas.edu.mx
- ⁷ Instituto Politécnico Nacional, CIIDIR Unidad Sinaloa, Guasave 81100, Mexico; moises_sm97@outlook.com
- * Correspondence: mespinoza1700@alumno.ipn.mx (M.E.O.); v_peinado@hotmail.com (V.M.P.G.); jherrera@cicese.mx (J.H.B.); jesuspeinado@uas.edu.mx (J.A.P.G.); Tel.: +52-687-102-7001 (M.E.O.); +52-687-107-3298 (V.M.P.G.); +52-646-126-0074 (J.H.B.); +52-687-857-8938 (J.A.P.G.)



Citation: Peinado Guevara, H.J.; Espinoza Ortiz, M.; Peinado Guevara, V.M.; Herrera Barrientos, J.; Peinado Guevara, J.A.; Delgado Rodríguez, O.; Pellegrini Cervantes, M.d.J.; Sánchez Morales, M. Potential Flood Risk in the City of Guasave, Sinaloa, the Effects of Population Growth, and Modifications to the Topographic Relief. *Sustainability* **2022**, *14*, 6560. <https://doi.org/10.3390/su14116560>

Academic Editors: Ayyoob Sharifi, Baojie He, Chi Feng and Jun Yang

Received: 25 April 2022

Accepted: 24 May 2022

Published: 27 May 2022

Publisher's Note: MDPI stays neutral with regard to jurisdictional claims in published maps and institutional affiliations.



Copyright: © 2022 by the authors. Licensee MDPI, Basel, Switzerland. This article is an open access article distributed under the terms and conditions of the Creative Commons Attribution (CC BY) license (<https://creativecommons.org/licenses/by/4.0/>).

Abstract: The coastal city of Guasave, Sinaloa, located on the Mexican Pacific coast, is subject to extreme precipitation events, which have caused flooding with damage to the city's infrastructure. The factors that influence flooding are vegetation, geology, degree of soil saturation, drainage characteristics of the watershed, and the shape of the topographic relief. Of the above factors, the topographic relief, which is the subject of the study, has been partially modified in some areas by infrastructure works (from 20.2 m to 17.6 m), and the population of the urban area has grown by 51.8% in 17 years (2004–2021); therefore, the objective is to evaluate the potential flood risk due to changes in this factor and the growth of the urban area. When using this method, the potential flood risk was determined considering four extreme events, 1982, 1990, 1998, and 2019. It was found that the potential risk increases for the whole city, being more intense in sector III, which, before the modification of the topographic relief, was the area with the lowest risk of flooding. In an extreme event such as Hurricane Paul in 1982, practically the entire city would be flooded.

Keywords: climate change; extraordinary floods; flood; high water; risk

1. Introduction

Urban population growth is a preponderant phenomenon for today's governments since it defines the direction of social policy in terms of safety and the provision of social welfare services. For a planned urban expansion, Getu and Bhat [1] consider those safe and sustainable policies and strategies should be adopted to avoid urban growth in hydrogeological risk areas.

Historically, the world's population has lived in rural environments, but the lack of economic opportunities in rural areas has led to accelerated migration and population growth toward urban environments [2]. Latin American and Caribbean countries are prone to hydro-meteorological natural disasters, which represent a threat to the population's

livelihoods and economic losses; in this context, the scientific analysis of the phenomenon allows providing relevant information linked to future climate and flood scenarios to anticipate potentially realistic preventive solutions [3]. Likewise, they require evaluations of the frequency and distribution of events for decision-making regarding urban expansion and the lack of efficient public policies [4]. Migration, population growth, and the lack of urban planning have generated informal and unstructured human settlements, which, in many cases, change land use with modifications to the topographic relief and environmental impacts, leading to alterations in the thermal, hydrological, and physical properties of the land surface [5–9]. These changes modify the flow path of surface runoff, increasing the risk of flooding [10] in urban areas, intensified by climate change, causing enormous human and infrastructure losses [11]. Lee et al. [12] propose a sustainable design strategy based on the concepts of robustness, speed, redundancy, and ingenuity to improve flood resilience.

In recent years, the issue of floods has generated greater awareness among decision-makers, especially due to extreme precipitation related to climate change, as they represent significant hazards, especially in urban areas where the population is settled [13–15]. The increase in these phenomena represents a serious threat to urban safety and sustainable development [16]. Ishiwatari and Sasaki [17] consider that, since one of the objectives of sustainable development is to invest in natural disaster risk reduction since natural disasters affect the development of towns by causing human and economic losses, then the limits of urban growth must be delineated. This has proven to be an effective route to avoiding hazardous situations [18].

Huang et al. [19] point out that urban planning is an issue that has been incorporated into the global sustainable development agenda. As an element of urban planning, urban storm flooding has attracted global attention [20]. This has led to the use of scientific models of urban expansion, such as the one mentioned in Al Rifat and Liu [21], with the urban growth prediction system. Lei et al. [22] suggest identifying flood-prone sites in urban environments, which, in the face of scarce hydraulic information, accurately map geographic susceptibility, seeking meaningful information to support government management decisions.

Data from geospatial information systems, maps, and remote sensing have become a useful tool for identifying recent and future urban growth patterns and assessing potential flood impacts, allowing authorities to plan and manage growth towards less risky areas and take effective mitigation measures [23–25].

Shrestha et al. [26] emphasize that the accuracy of hydrologic and hydrodynamic models used to study urban hydrology and predict urban flooding depends on the availability of data on installed infrastructure as well as the high resolution of topographic relief. This information is often lacking, thus motivating government decision-makers to improve risk management practices to substantially reduce the causes of flooding [27].

Urban flood risk mapping, future scenario planning for the directional management of urban growth, and risk assessment are resources that play a decisive role in political management and governance to face the challenges of climate change and flood risk [28–31]. Therefore, it is necessary to have instruments that authorities rely on to generate strategic logistics to conserve, divert and use flood flows [32].

The city of Guasave has been exposed to hurricanes and floods since its founding, until the most recent extreme event, Hurricane Isis, which flooded parts of the city of Guasave in 1998, even though the river and streams are regulated by dams and reservoirs upstream.

Due to extreme events, the Sinaloa River and Ocoroni Creek have overflowed, flooding the city of Guasave, Sinaloa in 1775, 1895, 1928, 1943, and 1958. In the 1943 and 1958 floods, the estimated discharge of the Sinaloa River was 3500 m³/s and 2500 m³/s, respectively [33].

Palafox et al. [34] have determined in the study area a return period of 25 years for intense floods, it has also indicated that the anthropogenic alterations in the topographic relief, the extraction of stone materials from the Sinaloa River, as well as the siltation of the

river channel, affect the intensity of the floods, without having determined the effect of the change in the topographic relief in the floods considering the urban growth.

Martínez [35] indicates that among the factors that influence the flood are the vegetation, geology, degree of soil saturation, drainage characteristics of the basin, and topographic relief form. In the case being analyzed, the topographical relief has undergone a quantifiable change, so when evaluating this change in the context of the growth of the urban sprawl, the potential risk of flooding is obtained.

Even though floods have occurred, the city continues to grow. The growth leads to modifications in the shape of the topographic relief and consequently of the direction of surface flow [36], which causes flooding in the city.

Then, considering the records of the water level elevation scales measured at the gauging station on the course of the Sinaloa River, the cost of the floods from 1976 to 2018, the quantification of the growth of the urban area, and the shape of the current topographic relief, so in this work, the objective is to determine the potential risk of a flood in the city due to changes in the topographic relief of the city considering the growth and distribution of the urban growth.

This study is fundamental for the development of public risk management and prevention policies that make life sustainable in the city of Guasave, Sinaloa, and in others where similar studies are carried out.

2. Materials and Methods

2.1. Description of the Study Area

The city of Guasave is located on a coastal plain of the Pacific Ocean, in the state of Sinaloa, northwestern Mexico, between coordinates $25^{\circ}31'29.97''$ and $25^{\circ}35'52.48''$ north latitude and $108^{\circ}26'33.7''$ to $108^{\circ}30'8.16''$ west longitude (see Figure 1). The city of Guasave has soils of alluvial origin from the Cenozoic Era and the Holocene period [37]. Its climate is dry, very warm, and hot, with summer rainfall and a mean annual temperature of 24.8°C for the 1986 to 2015 series. The average annual precipitation is 875.6 mm (1986 to 2016 series). Both data series correspond to the Jaina weather station, which is the closest to the city of Guasave [38].

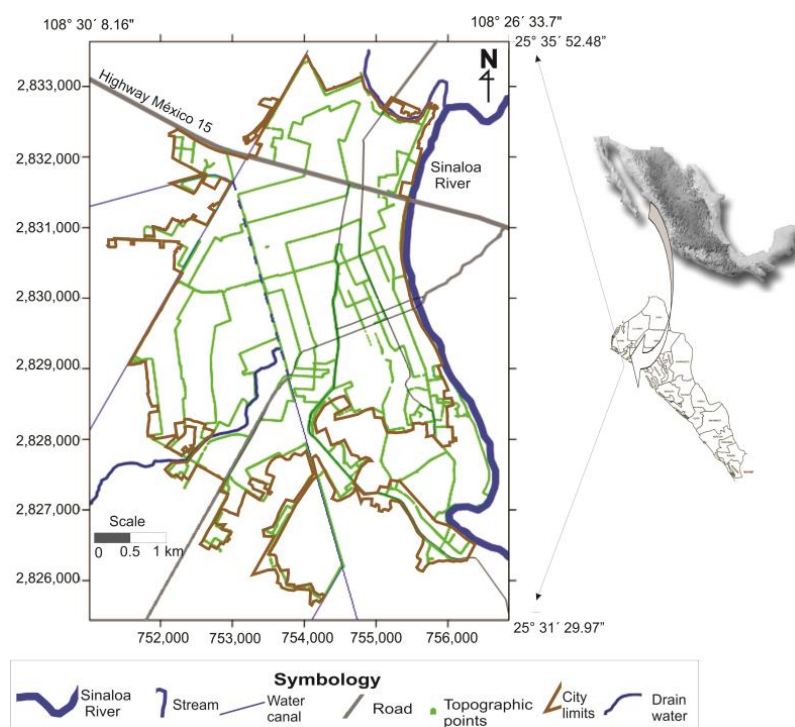


Figure 1. Location of the study area.

2.2. Growth of the Urban Layout

In order to determine the growth of the city, it was divided into seven areas whose perimeters are limited by the city contour, highways, canals, and main boulevards (Figure 2). From the nominal lists of the National Electoral Institute for the years 2004, 2007, 2009, 2012, 2015, and 2021, the location and number of people over 18 years of age in the different areas were obtained.

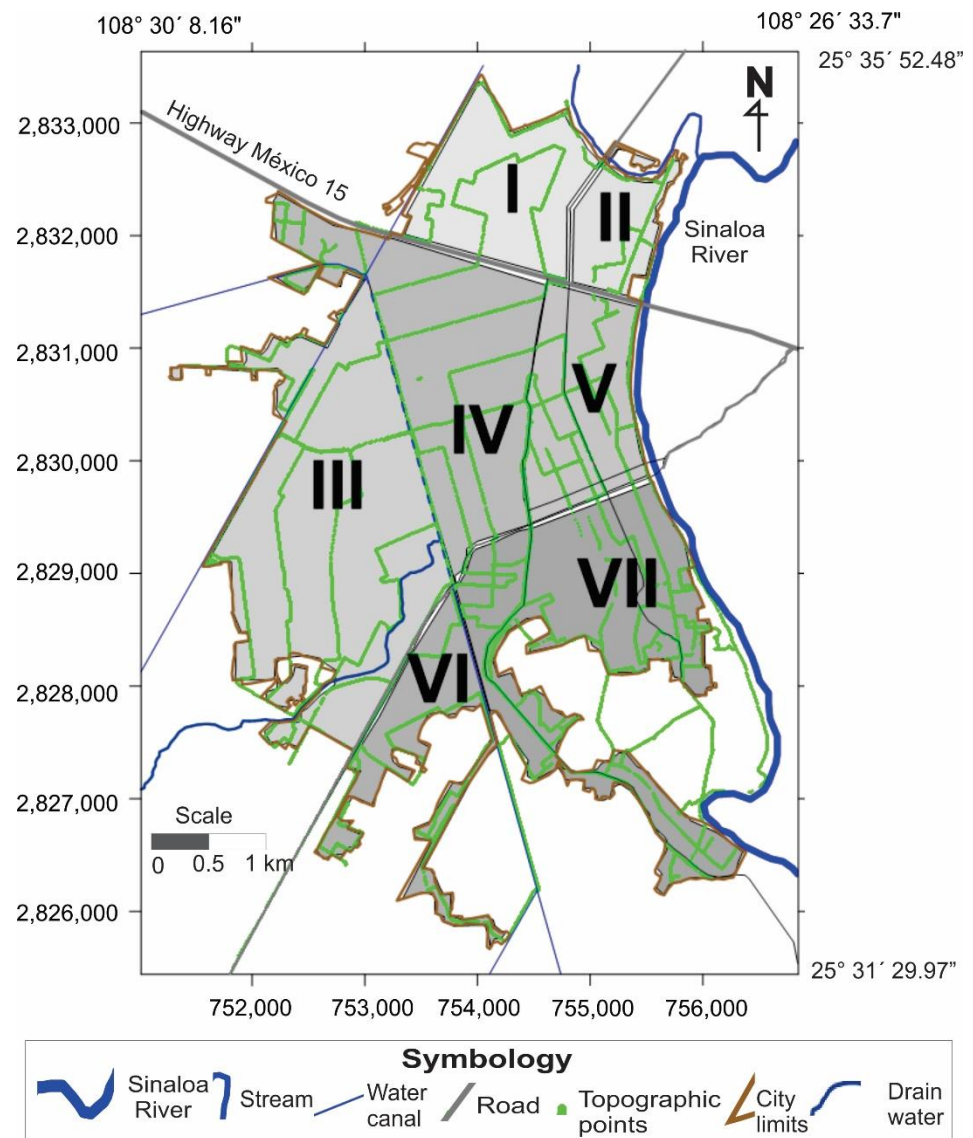


Figure 2. Division of the city of Guasave into 7 areas to monitor the population and territorial growth.

In order to determine the spatio-temporal growth of the city of Guasave, the population growth contour of the orthophoto of January 1994 G12D28E of INEGI [39] was digitized, as well as the contours of the historical satellite images of Google Earth Engine (GEE) for the years 2003, 2006, 2011, 2013 and 2020. Google Earth has applications in environmental and urban studies [40] with potential uses in fields such as human geography, geoscience education, and archaeology [41].

Google Earth images are basic for the determination of territorial growth, which coincides with the opinion of Taiema and Ramadan [23], who points out that geospatial and remote sensing information allows the identification of recent urban growth patterns. Likewise, it is important to analyze city growth trends and to take care of croplands as a source of food and income, as pointed out by Roy and Kasemi [5], who note that

urbanization processes modify the environment and economic and social profile of peri-urban areas. Likewise, Huang et al. [19] point out that it is necessary to make adjustments in land use policies in the face of the potential impact of urbanization, which makes sense since, in this study, agricultural areas are being affected.

2.3. Topographic Relief

The elevation of the terrain relief was obtained by precise GNSS positioning solution using an array of two SimpleRTK2B boards and two low-cost Arduosimple multiband antennas used in RTK (real-time kinematic) mode. The board contains the dual-frequency Ublox ZEP-F9P chip integrated, and an antenna is connected to it, so two configurations are made: board-antenna as transmitter and board-antenna as the receiver. The transmitting antenna is placed at a known coordinate point of the International Reference Frame ITRF08. The receiving antenna is placed on the roof of a car, and the data recorded by it are corrected using the NTRIP client protocol (Emlid Caster) via cellular internet connection. At each measurement point, the aim is to have the greatest satellite coverage and to have a FIX adjustment mode. In wooded areas or buildings, the recording periods were longer than in flat places, and, to achieve this adjustment, this RTK array was used because it is currently one of the most accurate real-time kinematic positioning methods [42,43].

The measurements obtained with the aforementioned instrument were checked against pre-existing geodetic measurements, as other authors have undertaken in geodetic applications [44–46], so this surveying equipment is centimeter-accurate, productive, and economical.

3. Results

3.1. Population Growth in the City of Guasave

Considering that the population census in Mexico is conducted every ten years and, provided the population dynamics, it is necessary to have counted in shorter periods to see how the population grows and is distributed in the territory. Regarding population growth, the electoral rolls were considered since, at least every three years, there are elections in the locality. The period from 2004 to 2021 was considered, that is, a period of 17 years. In that period, the electoral roll increased by 32.83%. In the city, the increase was 51.82%, congruent with Henríquez et al. [2]. The current demographic trend is to live in urban environments. Considering the seven areas into which the city was divided, there are differences among them, so that in zone III, the growth was 235.2%, followed by zone VI with 80.69% (See Table 1).

Table 1. Population growth considering the nominal list of the National Electoral Institute (INE), period 2004–2021.

Area	2004	2007	2009	2012	2015	2021
I	4972 0	5484 10.30%	5849 17.64%	6628 33.31%	7184 44.49%	8537 71.70%
II	3040 0	3156 3.82%	3191 4.97%	3931 29.31%	3118 2.57%	4602 51.38%
III	4767 0	6082 27.59%	7120 49.36%	9693 103.34%	11,901 149.65%	15,979 235.20%
IV	12,343 0	12,490 1.19%	12,495 1.23%	12,823 3.89%	11,571 −6.25%	14,013 13.53%
V	9227 0	9129 −1.06%	9005 −2.41%	8492 −7.97%	7999 −13.31%	9259 0.35%
VI	1186 0	1299 9.53%	1395 17.62%	1540 29.85%	1510 27.32%	2143 80.69%
VII	6546 0	6845 4.57%	7050 7.70%	7456 13.90%	7944 21.36%	9354 42.90%

Table 1. Cont.

Area	2004	2007	2009	2012	2015	2021
City	42,081 0	44,485 5.71%	46,105 9.56%	50,563 20.16%	51,227 21.73%	63,887 51.82%
Municipality	176,426 0	183,478 4.00%	190,048 7.72%	199,663 13.17%	199,650 13.16%	234,350 32.83%

3.2. Territorial Growth of the City of Guasave

By superimposing the contours of the 1994 INEGI orthophoto with those of the historical images of the Google Earth application, the spatial and temporal variation of the growth of the city of Guasave was obtained (see Figure 3). Population growth extends to the west and southwest of the city, which coincides with the increase in population reflected in the nominal lists.

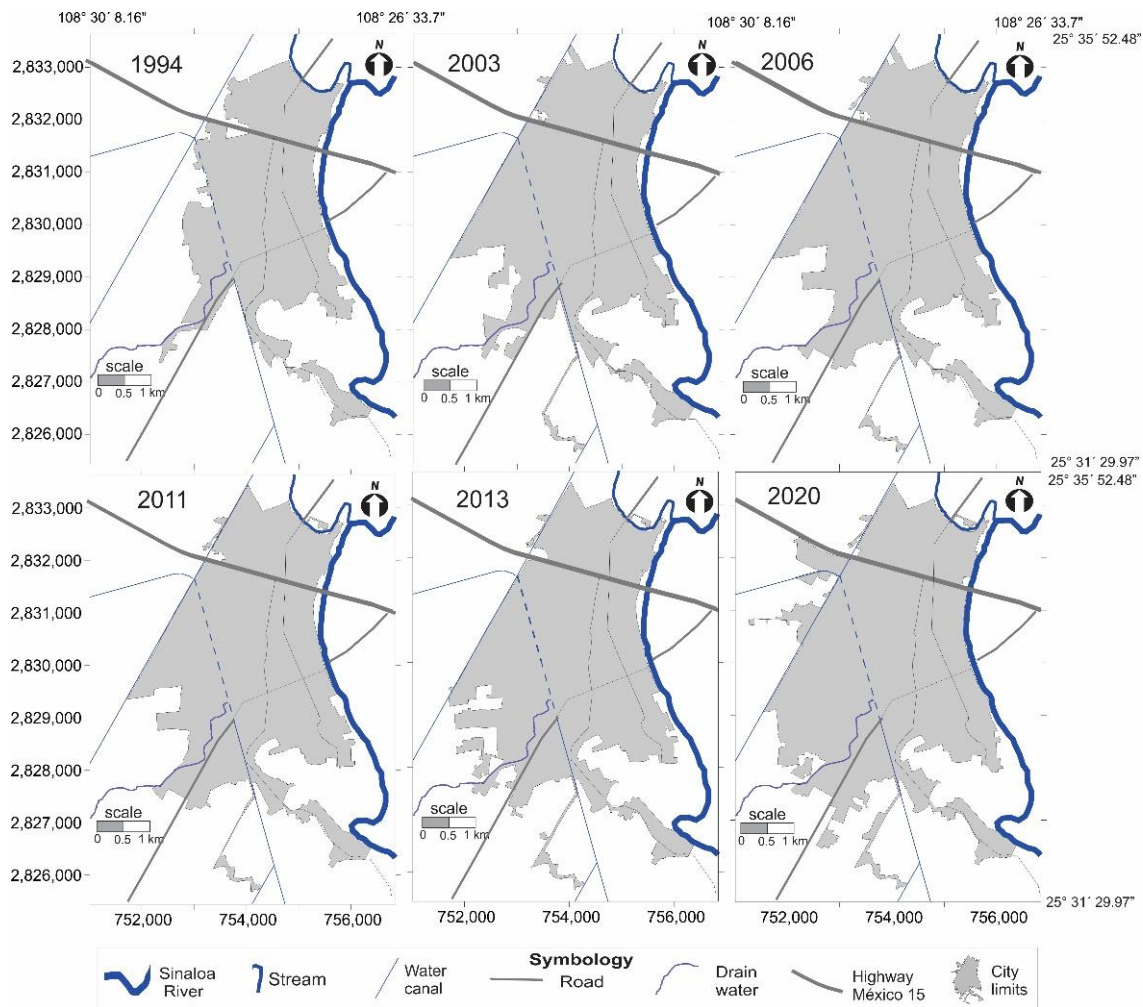


Figure 3. Territorial growth trend of the city of Guasave.

The correlation coefficient between the variables time and urban land area is $r = 0.985$ (see Figure 4). The equation that justifies this coefficient is:

$$A = 241,453t - 46.96 \times 10^7 \tag{1}$$

where A is the area in m^2 and t is the time in years.

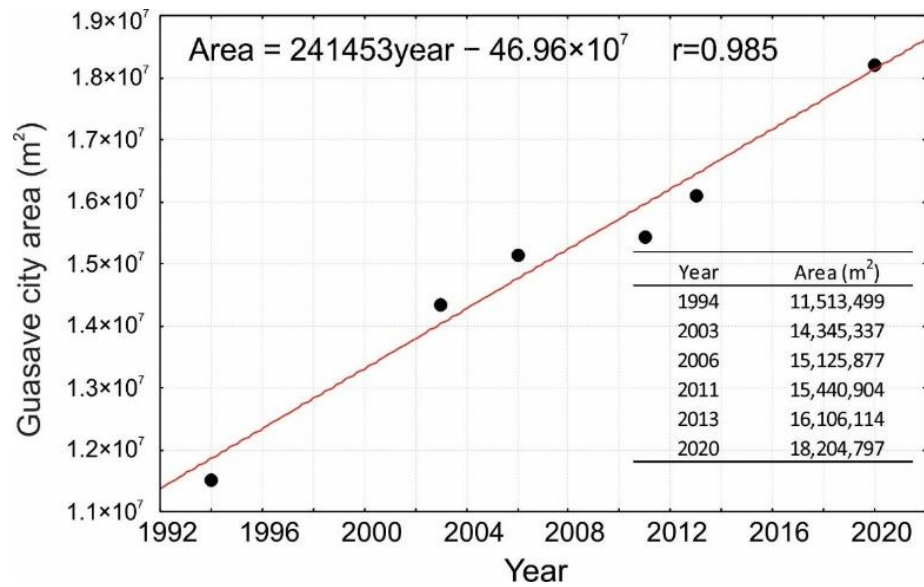


Figure 4. Relationship between the territorial area of the city and the time.

From the slope of this graph, the city grows at a rate of 25 hectares per year.

Figure 5 shows the territorial expansion over time, showing that the city is growing in and towards agricultural land, which, if this growth trend continues, could jeopardize the municipality’s food security.

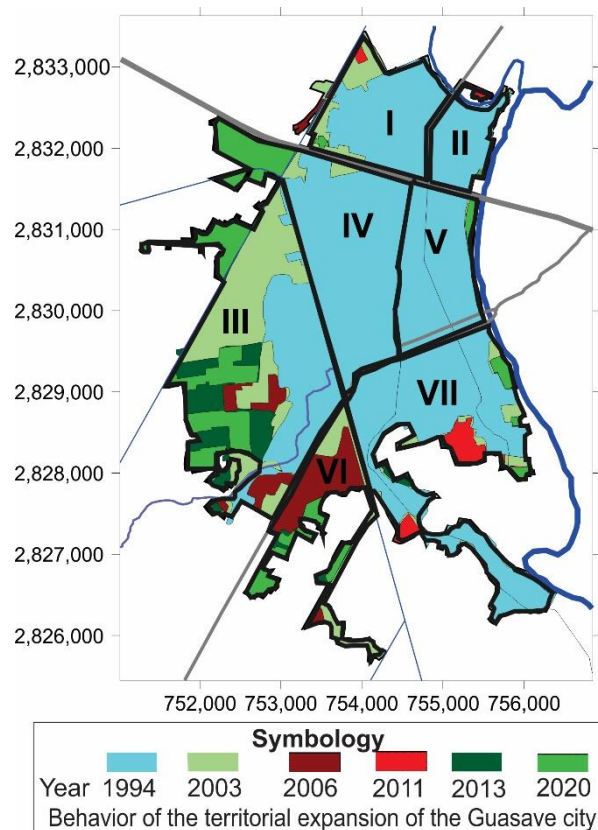


Figure 5. Territorial expansion of the city of Guasave over the years.

3.3. Topographic Relief

The topographic relief, which is the subject of the study, has been partially modified in some areas by infrastructure works. In 2012 the work of piping the canal that divided areas III and IV was completed, modifying the topographic relief so that the height of the terrain changed at the boundary; before the piping, the height varied from 17.6 m to 20.2 m; with the piping, the height ranges from 16.4 to 18.8 m, leaving sector III vulnerable to flooding. The section of the topographic relief that was modified by this work is approximately 3 km long.

3.4. Flood Risks

The National Water Commission, through the North Pacific Regional Management and Irrigation District 063, provided information on the maximum extraordinary floods of the Sinaloa River, see Table 2. Columns two and three show the heights of the water level, referred to as mean sea level (m.a.s.l.), the scales, as well as the Sinaloa River discharge. These data correspond to the gauging station, Jaina, located at the toll bridge on the Mexico 15 international highway.

Table 2. Record of extraordinary floods on the Sinaloa River as it passes through the city of Guasave.

Date	Scale m.a.s.l.	Outflow m ³ /s	Hydro Climatological Phenomenon
2 October 1976	15.89	1520.00	Extraordinary Rainfall
3 September 1978	15.66	1259.00	Extraordinary Rainfall
4 September 1979	16.66	1825.00	Extraordinary rainfall
5 August 1980	15.25	1265.00	Extraordinary rainfall
10 October 1981	17.35	2228.30	Hurricane Norma
2 October 1982	18.05	2826.00	Hurricane Paul
9 August 1984	15.82	1367.20	Extraordinary Rainfall
10 August 1985	14.01	577.00	Extraordinary rainfall
3 October 1986	15.78	748.20	Hurricane Payne
12 July 1990	15.72	771.00	Extraordinary Rainfall
12 December 1990	15.60	723.00	Extraordinary Rainfall
26 September 1991	14.15	315.00	Extraordinary Rainfall
25 December 1991	14.36	350.00	Extraordinary Rainfall
27 January 1992	15.07	472.00	Extraordinary Rainfall
14 September 1993	14.90	444.00	Extraordinary Rainfall
14 November 1994	16.24	969.00	Extraordinary Rainfall
16 September 1995	15.24	510.00	Hurricane Ishmael
15 September 1996	15.51	599.20	Hurricane Fausto
4 September 1998	17.60	1798.00	Hurricane Isis
21 September 2015	14.94	426.000	Extraordinary Rainfall
22 September 2018	14.93	412.440	Extraordinary Rainfall

Figure 6 shows the relationship between the water level height of the Sinaloa River versus discharge at the gauging station mentioned above. This was obtained with 617 observations for the period 2012–2020. The correlation coefficient for this series is $r = 0.969$, and the relationship is:

$$Q = 0.264 \times 10^{-6} h^{7.97619} - 5.55 \quad (2)$$

where Q is the discharge in m³/s and h is the height in meters above mean sea level.

This equation indicates that an increase in h is associated with an increase in Q and vice versa. The scale varies from 14.01 to 18.05 m over 42 years, with a mean value of 15.65 m.

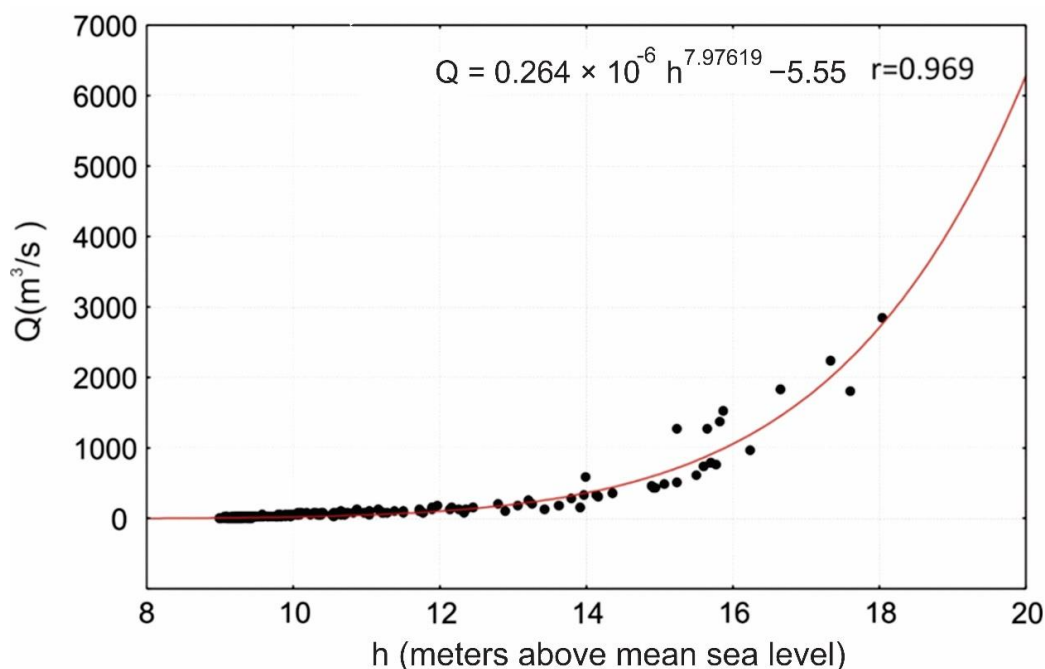


Figure 6. The relationship between discharge and height reached at the gauging station on the Sinaloa River at the bridge over the Mexico 15 international highway.

3.5. Possible Causes

Considering the current topographic relief configuration and the assumption that extreme precipitation events are to be repeated, Figure 6 shows four possible scenarios of potential flood risks for the city of Guasave and its immediate surroundings.

In 2018 the water level of the Sinaloa River reached 14.93 m high, with an outflow of 412.44 m³/s. With that height, it is observed in Figure 7A that the southwest of the city would be affected. It is worth mentioning that when this event occurred, sector III was not flooded due to the presence of the channel, which to date has been piped in a portion of approximately 3 km.

On 12 July 1990, the water level of the Sinaloa River reached a height of 15.72 m with a discharge of 777.1 m³/s. Figure 7B shows that with that elevation, the water level would reach the urban area of the city.

On 4 September 1998, Hurricane Isis generated a water flow that reached a height of 17.6 m with a discharge of 1798 m³/s. This affected neighborhoods in the city. This affected neighborhoods in the city of Guasave. It is important to note that area III was not affected because the channel described above passed between areas III and IV. If this extreme event were to occur again, so that the water reaches a height of 17.6 m, areas III, IV, VI, and VII would be affected, i.e., area III would be included, see Figure 7C.

On 2 October 1982, Hurricane Paul generated a flow of water that reached a height of 18.05 m and a flow rate of 2826 m³/s. In the event of a repetition of this storm and reaching the height of 18.05 m, with the current topographic relief, most of the city of Guasave would be flooded, see Figure 7D.

With the information provided by the Guasave City Hall [33], it was possible to identify the territorial extension flooded by Hurricane Isis in 1998. The affected areas were digitized, see Figure 8A. Note that zone III was protected from flooding by the presence of the canal. If a phenomenon similar to that of 1998 were to occur again, the potential risk of flooding would increase, especially in the eastern and southeastern sectors, due to the absence of the canal.

The probability of a recurrence of a phenomenon such as Hurricane Isis is high since in the studies carried out by Palafox Avila [36], upon analyzing the maximum water discharge over the Sinaloa River using the log-Pearson type III and Gumbel models, he concluded

that the probability of a recurrence of a discharge such as that of 1998 for the next 25 years is 96% and for the next 50 years it is 98%.

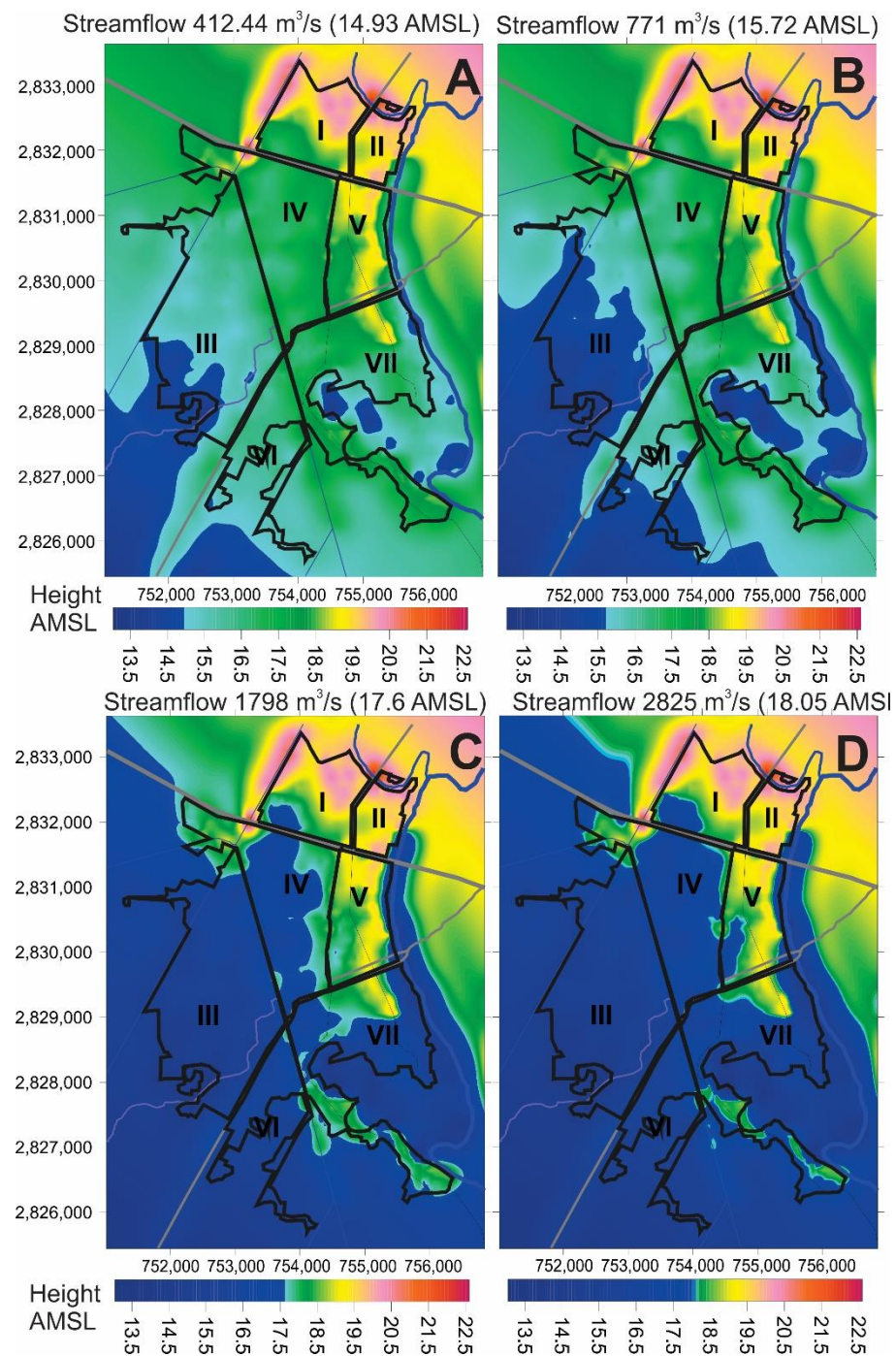


Figure 7. Flood scenarios in the event of extraordinary floods according to CONAGUA records. Possible flood scenarios based on current topographic relief with the streamflow in the Sinaloa River of (A) 412 m³/s, (B) 771 m³/s, (C) 1798 m³/s and (D) 2825 m³/s.

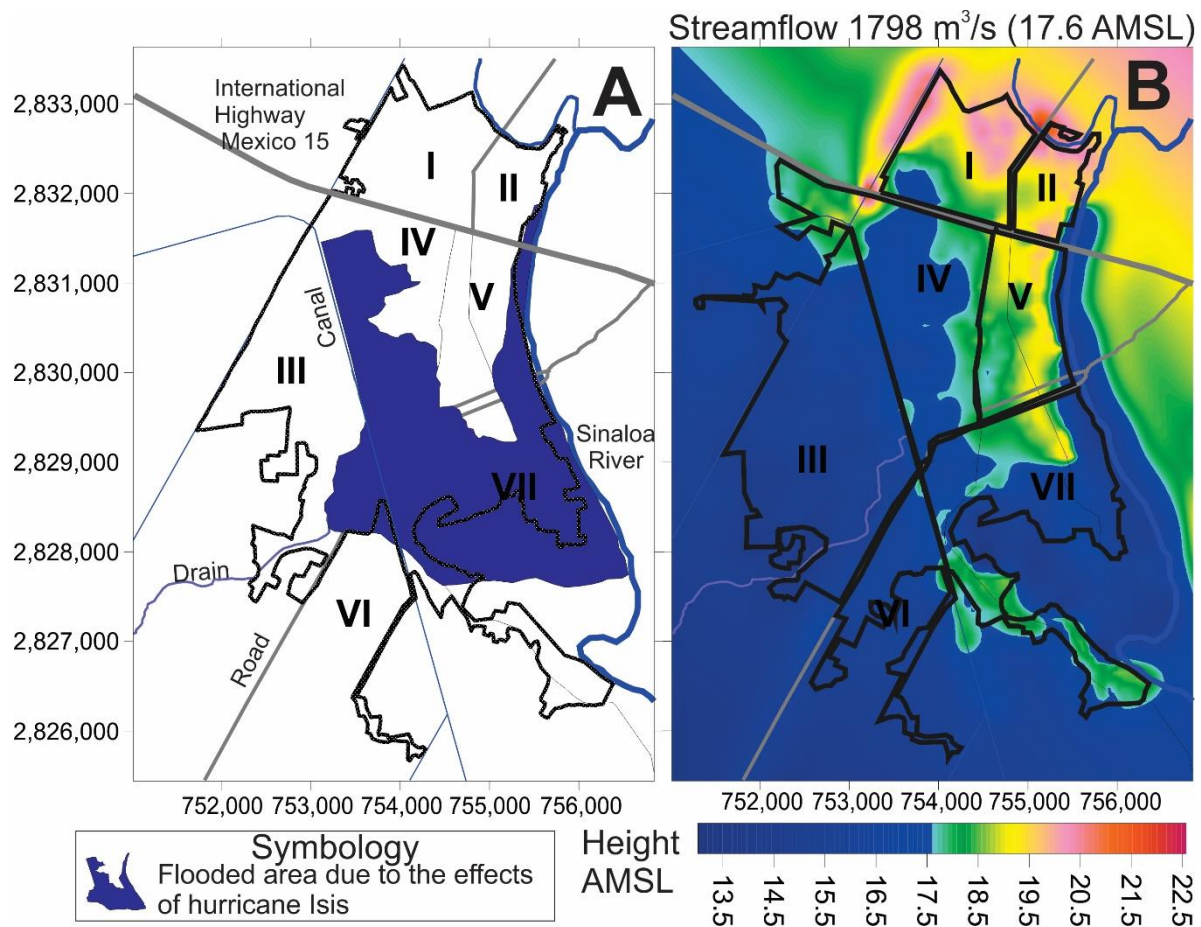


Figure 8. Comparison between the impact in the event of a repetition of an extraordinary flood such as the one in 1998 with hurricane Isis. (A) flooded area in the city of Guasave in 1998, (B) New scenario considering current conditions.

In the images shown in Figure 9, two cross-sections of the river can be seen. Profile one shows the behaviour of the slope of the terrain, which as it moves away from the right bank of the Sinaloa River, its height decreases; likewise, it can be seen that with the piping of the canal that passes through the city of Guasave, the height of the pipe practically coincides with that of the terrain. On the other hand, profile two shows a low point in the central part, where water from the Sinaloa River could enter the city in the event of an extraordinary flood. The prolongation of the canal that can be seen constituted artificial protection to sector III of the city.

The images shown in Figure 9 show profiles one and two transversal to the river, as well as profile three parallel to the river. Profile one shows that as it moves away from the right bank of the Sinaloa River, its height decreases; likewise, it can be seen that with the canal piping that passes through the city of Guasave, the height of the terrain practically maintains the same elevation. On the other hand, profile two shows a low point in the central part, where water from the Sinaloa River could enter the city in an extraordinary flood, depending on the amount of water passing through at that time. This profile also shows a channel that acts as artificial protection to sector VI of the city.

Profile three of Figure 9 shows the current topographic relief of the city of Guasave and, with dotted lines (inferred from some remnants), shows the level before the canal was piped through the city. The current relief generates conditions of potential flood risk in zones III and VI due to the decrease in the height of the topographic relief.

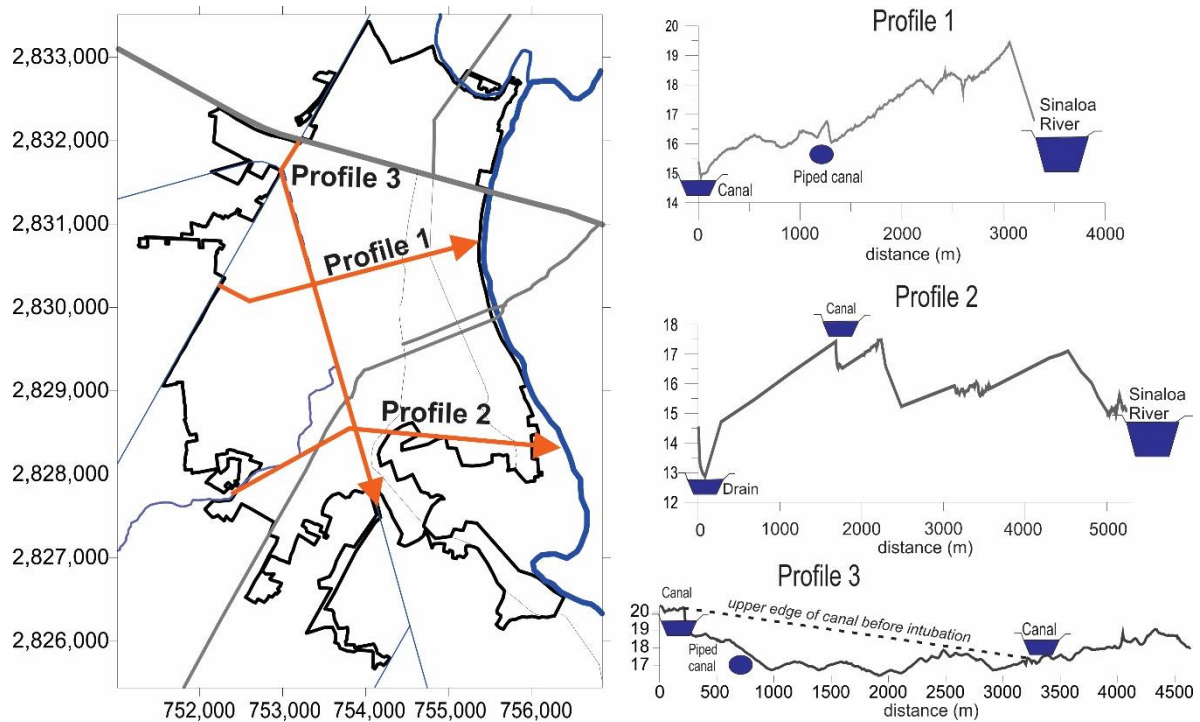


Figure 9. Transverse and parallel profiles to the Sinaloa River.

4. Discussion

In addition to the natural causes of floods [47], there are anthropogenic causes such as modifications to the topographic relief and the growth of urbanization of the land. These two factors have been considered in this work as elements in the potential risk of flooding caused by extreme events. Efforts are also being made in other latitudes to reduce the effects of floods caused by floods.

Poku-Boansi et al. [13] state that recent years have been characterized by a greater awareness of flood hazards and other natural disasters. Lei et al. [22] consider that it is necessary to identify sites vulnerable to floods in urban environments to mitigate their effects. Dumedah et al. [10] recommend that intervention efforts and the creation of adequate spaces for water to flow during a flood should be promoted.

Kiss et al. [48], when studying floods in a confined floodplain river in Lower Tisza, Hungary, found that to mitigate the effects of a flood, riverine vegetation should be properly managed since it influences the speed and duration of flooding, and recommends placing artificial works to increase the height at crucial points.

Osei et al. [49] studied return periods using Gumbel's extreme value theory with data from the Pra River in Ghana, West Africa, to evaluate future flood risks, recommending the construction of hydraulic structures such as dams and reservoirs to adapt to flooding in the basin. In this work, we used the calculations on return periods of Palafox Avila, [36], who uses the Gumbel function and log-Pearson type III, finding that the extreme event of 1998 can occur every 25 years with a probability of 96%.

Bang and Burton [50] conducted a study on flooding problems by the River Steeping in England to know the contemporary perception of flood risk, conducting surveys to the population which indicated that it is important to provide regular maintenance/reinforcement of flood defenses, construction of more levees/terraces along the River Steeping, greater awareness/knowledge of the community and responsibility among others.

Thapa et al. [51] assessed flood hazards from frequent flooding of the Khandu River basin in eastern Nepal using 47 years of rainfall data and estimated the water column thickness of a flood for the basin. From return periods of 20, 50, 100, and 200 years

they generated flood risk maps as well as floodwater column thickness, thus creating vulnerability and fragility functions. In this work, flood thicknesses were also generated, as well as flood surfaces framed by sectors, as well as the flood risks of the city in the face of four potential events, that is, the efforts to identify flood risk or danger zones are efforts that are made in different latitudes under the considerations of each place or region, in this work the importance of the anthropogenic modification to the topographic relief and the growth of urbanization zones for residential use has been emphasized.

5. Conclusions

The potential flood risk of the city of Guasave in the face of possible extreme events was determined. The risks of the six sections into which the city was divided were determined differentially. The anthropogenic variables causing the risk of flooding were considered as modifications to the topographic relief, as well as the rate of urban growth of the city without considering the shape of the topographic relief, that is, without having previously identified the areas of greatest risk of flooding. The growth of urbanization was determined for 17 years from historical images, finding that it grows at a rate of 25 hectares per year. Growth is asymmetric and tends to occupy agricultural land on the right bank of the Sinaloa River. The population in 17 years has grown by 30%. From the point of view of the six sectors, population growth is heterogeneous, with some growing more than twice as fast. The growth is towards the eastern and southwestern portions, and this is corroborated with information from the INE (National Electoral Institute). On the other hand, due to modifications to the topographic relief of sector III, it became vulnerable to flooding; likewise, in general, the potential risk of flooding increased for the city due to the additive effect of population growth and modifications to the topographic relief.

Author Contributions: Conceptualization, H.J.P.G., M.E.O., V.M.P.G. and J.H.B.; methodology, H.J.P.G., M.E.O. and J.H.B.; software, H.J.P.G. and M.S.M.; validation, J.H.B. and V.M.P.G.; formal analysis, J.A.P.G., O.D.R. and M.d.J.P.C.; investigation, H.J.P.G., V.M.P.G. and J.A.P.G.; resources, H.J.P.G. and V.M.P.G.; data curation, O.D.R., M.d.J.P.C. and M.S.M.; writing—original draft preparation, H.J.P.G., V.M.P.G. and J.H.B.; writing—review and editing, M.E.O., J.A.P.G., O.D.R. and M.d.J.P.C.; visualization, H.J.P.G. and M.S.M.; supervision, J.A.P.G., O.D.R. and M.d.J.P.C.; project administration, H.J.P.G., M.E.O. and J.H.B.; funding acquisition, H.J.P.G., V.M.P.G. and J.A.P.G. All authors have read and agreed to the published version of the manuscript.

Funding: This research received no external funding.

Institutional Review Board Statement: Not applicable.

Acknowledgments: To CONACYT for the fellowship received by the student Mauro Espinoza Ortiz and Moisés Sánchez Morales.

Conflicts of Interest: The authors declare no conflict of interest. The funders had no role in the design of the study; in the collection, analyses, or interpretation of data; in the writing of the manuscript, or in the decision to publish the results.

References

1. Getu, K.; Bhat, H.G. Analysis of spatio-temporal dynamics of urban sprawl and growth pattern using geospatial technologies and landscape metrics in Bahir Dar, Northwest Ethiopia. *Land Use Policy* **2021**, *109*, 105676. [[CrossRef](#)]
2. Henríquez, C.; Azócar, G.; Romero, H. Monitoring and modeling the urban growth of two mid-sized Chilean cities. *Habitat Int.* **2006**, *30*, 945–964. [[CrossRef](#)]
3. Pinos, J.; Quesada-Román, A. Flood Risk-Related Research Trends in Latin America and Caribbean. *Water* **2021**, *14*, 10. [[CrossRef](#)]
4. Quesada-Román, A.; Villalobos-Portilla, E.; Campos-Durán, D. Hydrometeorological disasters in urban areas of Costa Rica, Central America. *Environ. Hazards* **2020**, *20*, 264–278. [[CrossRef](#)]
5. Roy, B.; Kasemi, N. Monitoring urban growth dynamics using remote sensing and GIS techniques of Raiganj Urban Agglomeration, India. *Egypt. J. Remote Sens. Space Sci.* **2021**, *24*, 221–230. [[CrossRef](#)]
6. Xian, G.; Shi, H.; Zhou, Q.; Auch, R.; Gallo, K.; Wu, Z.; Kolian, M. Monitoring and characterizing multi-decadal variations of urban thermal condition using time-series thermal remote sensing and dynamic land cover data. *Remote Sens. Environ.* **2021**, *269*, 112803. [[CrossRef](#)]

7. Dutta, D.; Rahman, A.; Paul, S.; Kundu, A. Impervious surface growth and its inter-relationship with vegetation cover and land surface temperature in peri-urban areas of Delhi. *Urban Clim.* **2021**, *37*, 100799. [[CrossRef](#)]
8. Flores, A.P.; Giordano, L.; Ruggerio, C.A. A basin-level analysis of flood risk in urban and periurban areas: A case study in the metropolitan region of Buenos Aires, Argentina. *Heliyon* **2020**, *6*, e04517. [[CrossRef](#)]
9. Hegazy, I.R.; Kaloop, M.R. Monitoring urban growth and land use change detection with GIS and remote sensing techniques in Daqahlia governorate Egypt. *Int. J. Sustain. Built Environ.* **2015**, *4*, 117–124. [[CrossRef](#)]
10. Dumedah, G.; Andam-Akorful, S.A.; Ampofo, S.T.; Abugri, I. Characterizing urban morphology types for surface runoff estimation in the Oforikrom Municipality of Ghana. *J. Hydrol. Reg. Stud.* **2021**, *34*, 100796. [[CrossRef](#)]
11. Zhu, S.; Li, D.; Huang, G.; Chhipi-Shrestha, G.; Nahiduzzaman, K.M.; Hewage, K.; Sadiq, R. Enhancing urban flood resilience: A holistic framework incorporating historic worst flood to Yangtze River Delta, China. *Int. J. Disaster Risk Reduct.* **2021**, *61*, 102355. [[CrossRef](#)]
12. Lee, H.; Song, K.; Kim, G.; Chon, J. Flood-adaptive green infrastructure planning for urban resilience. *Landsc. Ecol. Eng.* **2021**, *17*, 427–437. [[CrossRef](#)]
13. Poku-Boansi, M.; Amoako, C.; Owusu-Ansah, J.K.; Cobbinah, P.B. What the state does but fails: Exploring smart options for urban flood risk management in informal Accra, Ghana. *City Environ. Interact.* **2020**, *5*, 100038. [[CrossRef](#)]
14. Avashia, V.; Garg, A. Implications of land use transitions and climate change on local flooding in urban areas: An assessment of 42 Indian cities. *Land Use Policy* **2020**, *95*, 104571. [[CrossRef](#)]
15. Mohtar, W.H.M.W.; Abdullah, J.; Maulud, K.N.A.; Muhammad, N.S. Urban flash flood index based on historical rainfall events. *Sustain. Cities Soc.* **2020**, *56*, 102088. [[CrossRef](#)]
16. Wang, P.; Li, Y.; Yu, P.; Zhang, Y. The analysis of urban flood risk propagation based on the modified susceptible infected recovered model. *J. Hydrol.* **2021**, *603*, 127121. [[CrossRef](#)]
17. Ishiwatari, M.; Sasaki, D. Investing in flood protection in Asia: An empirical study focusing on the relationship between investment and damage. *Prog. Disaster Sci.* **2021**, *12*, 100197. [[CrossRef](#)]
18. Liu, X.; Wei, M.; Li, Z.; Zeng, J. Multi-scenario simulation of urban growth boundaries with an ESP-FLUS model: A case study of the Min Delta region, China. *Ecol. Indic.* **2022**, *135*, 108538. [[CrossRef](#)]
19. Huang, X.; Wang, H.; Xiao, F. Simulating urban growth affected by national and regional land use policies: Case study from Wuhan, China. *Land Use Policy* **2021**, *112*, 105850. [[CrossRef](#)]
20. Luo, K.; Zhang, X. Increasing urban flood risk in China over recent 40 years induced by LUCC. *Landsc. Urban Plan.* **2022**, *219*, 104317. [[CrossRef](#)]
21. Al Rifat, S.A.; Liu, W. Predicting future urban growth scenarios and potential urban flood exposure using Artificial Neural Network-Markov Chain model in Miami Metropolitan Area. *Land Use Policy* **2022**, *114*, 105994. [[CrossRef](#)]
22. Lei, X.; Chen, W.; Panahi, M.; Falah, F.; Rahmati, O.; Uemaa, E.; Kalantari, Z.; Ferreira, C.S.S.; Rezaie, F.; Tiefenbacher, J.P.; et al. Urban flood modeling using deep-learning approaches in Seoul, South Korea. *J. Hydrol.* **2021**, *601*, 126684. [[CrossRef](#)]
23. Taiema, F.S.; Ramadan, M.S. Monitoring urban growth directions using geomatics techniques, a case study Zagazig city-Egypt. *Egypt. J. Remote Sens. Space Sci.* **2021**, *24*, 1083–1092. [[CrossRef](#)]
24. Salvati, P.; Ardizzone, F.; Cardinali, M.; Fiorucci, F.; Fugnoli, F.; Guzzetti, F.; Marchesini, I.; Rinaldi, G.; Rossi, M.; Santangelo, M.; et al. Acquiring vulnerability indicators to geo-hydrological hazards: An example of mobile phone-based data collection. *Int. J. Disaster Risk Reduct.* **2021**, *55*, 102087. [[CrossRef](#)]
25. Rana, S.; Sarkar, S. Prediction of urban expansion by using land cover change detection approach. *Heliyon* **2021**, *7*, e08437. [[CrossRef](#)]
26. Shrestha, A.; Mascaro, G.; Garcia, M. Effects of stormwater infrastructure data completeness and model resolution on urban flood modeling. *J. Hydrol.* **2022**, *607*, 127498. [[CrossRef](#)]
27. da Silva, L.B.L.; Alencar, M.H.; de Almeida, A.T. A novel spatiotemporal multi-attribute method for assessing flood risks in urban spaces under climate change and demographic scenarios. *Sustain. Cities Soc.* **2022**, *76*, 103501. [[CrossRef](#)]
28. Eini, M.; Kaboli, H.S.; Rashidian, M.; Hedayat, H. Hazard and vulnerability in urban flood risk mapping: Machine learning techniques and considering the role of urban districts. *Int. J. Disaster Risk Reduct.* **2020**, *50*, 101687. [[CrossRef](#)]
29. Kim, Y.; Newman, G. Advancing scenario planning through integrating urban growth prediction with future flood risk models. *Comput. Environ. Urban Syst.* **2020**, *82*, 101498. [[CrossRef](#)]
30. Papilloud, T.; Röthlisberger, V.; Loreti, S.; Keiler, M. Flood exposure analysis of road infrastructure—Comparison of different methods at national level. *Int. J. Disaster Risk Reduct.* **2020**, *47*, 101548. [[CrossRef](#)]
31. Flores, C.C.; Vikolainen, V.; Cromptvoets, J. Governance assessment of a blue-green infrastructure project in a small size city in Belgium. The potential of Herentals for a leapfrog to water sensitive. *Cities* **2021**, *117*, 103331. [[CrossRef](#)]
32. Jain, S.K. Providing water security in India by conserving and utilizing flood flows. *Water Secur.* **2021**, *14*, 100105. [[CrossRef](#)]
33. Rubio, R.H. *Guasave, Historia de un Pueblo Primera*; Universidad Autonoma de sinaloa: Culiacán Rosales, Mexico, 2015.
34. Palafox-Ávila, G.; Barrientos, J.H.; Ladrón-de-Guevara Torres, M.A.; Guevara, H.J.P.; Guevara, L.I.P.; de Campos, J.J.G. Riesgos potenciales de inundaciones en la ciudad de Guasave, Sinaloa. In *Sinaloa Ante El Cambio Climático Global*; Primera, L.M., Campaña, R.E.F., Angulo, C.M., Quiñonez, K., Eds.; Universidad Autónoma de Sinaloa: Culiacán Rosales, Mexico, 2014; pp. 145–165.

35. Goytre, J.M. Las Avenidas: Un proceso geológico natural. In *Cursos de Ingeniería Geoambiental*; Instituto Geológico y Minero de España: Madrid, España, 1990; pp. 1–20.
36. Ávila, G.P. *Riesgo Potencial a Inundaciones en la Ciudad De Guasave*; Instituto Politécnico Nacional: Sinaloa, Mexico, 2006.
37. INEGI. *Guasave Sinaloa, Cuaderno Estadístico Municipal*, 1st ed.; Instituto Nacional de Estadística, Geografía e Informática: Aguascalientes, Mexico, 2000; 192p.
38. INEGI. *Anuario estadístico y geográfico de Sinaloa 2017*; Instituto Nacional de Estadística, Geografía e Informática: Aguascalientes, Mexico, 2017; 475p.
39. INEGI. Ortofoto Digital: G12D28E. 1994. Available online: <https://www.inegi.org.mx/app/biblioteca/ficha.html?upc=889463460923> (accessed on 15 January 2022).
40. Liang, J.; Xie, Y.; Sha, Z.; Zhou, A. Modeling urban growth sustainability in the cloud by augmenting Google Earth Engine (GEE). *Comput. Environ. Urban Syst.* **2020**, *84*, 101542. [[CrossRef](#)]
41. Liang, J.; Gong, J.; Li, W. Applications and impacts of Google Earth: A decadal review (2006–2016). *ISPRS J. Photogramm. Remote Sens.* **2018**, *146*, 91–107. [[CrossRef](#)]
42. Olivart, I.; Llop, J.O.; Moreno-Salinas, D.; Sánchez, J. Full Real-Time Positioning and Attitude System Based on GNSS-RTK Technology. *Sustainability* **2020**, *12*, 9796. [[CrossRef](#)]
43. Prochniewicz, D.; Szpunar, R.; Walo, J. A new study of describing the reliability of GNSS Network RTK positioning with the use of quality indicators. *Meas. Sci. Technol.* **2017**, *28*, 15012. [[CrossRef](#)]
44. Hamza, V.; Stopar, B.; Ambrožič, T.; Turk, G.; Sterle, O. Testing Multi-Frequency Low-Cost GNSS Receivers for Geodetic Monitoring Purposes. *Sensors* **2020**, *20*, 4375. [[CrossRef](#)]
45. Hamza, V.; Stopar, B.; Sterle, O. Testing the Performance of Multi-Frequency Low-Cost GNSS Receivers and Antennas. *Sensors* **2021**, *21*, 2029. [[CrossRef](#)]
46. Hodgson, M.E. On the accuracy of low-cost dual-frequency GNSS network receivers and reference data. *GISci. Remote Sens.* **2020**, *57*, 907–923. [[CrossRef](#)]
47. Karamouz, M.; Ahmadi, A.; Akhbari, M. Groundwater Risk and Disaster Management. In *Ground Water Hydrology. Engineering, Planning, and Management*; CRC Press: Boca Raton, FL, USA, 2011; p. 11.
48. Kiss, T.; Nagy, J.; Fehérvári, I.; Amisshah, G.J.; Fiala, K.; Sipos, G. Increased flood height driven by local factors on a regulated river with a confined floodplain, Lower Tisza, Hungary. *Geomorphology* **2021**, *389*, 107858. [[CrossRef](#)]
49. Osei, M.A.; Amekudzi, L.K.; Omari-Sasu, A.Y.; Yamba, E.I.; Quansah, E.; Aryee, J.N.; Preko, K. Estimation of the return periods of maxima rainfall and floods at the Pra River Catchment, Ghana, West Africa using the Gumbel extreme value theory. *Heliyon* **2021**, *7*, e06980. [[CrossRef](#)] [[PubMed](#)]
50. Bang, H.N.; Burton, N.C. Contemporary flood risk perceptions in England: Implications for flood risk management foresight. *Clim. Risk Manag.* **2021**, *32*, 100317. [[CrossRef](#)]
51. Thapa, S.; Shrestha, A.; Lamichhane, S.; Adhikari, R.; Gautam, D. Catchment-scale flood hazard mapping and flood vulnerability analysis of residential buildings: The case of Khando River in eastern Nepal. *J. Hydrol. Reg. Stud.* **2020**, *30*, 100704. [[CrossRef](#)]